NUMERICAL SIMULATION OF HOMOGENOUS/INHOMOGENEOUS HYD ROGEN-AIR EXPLOSION IN A LONG CLOSED CHANNEL

Qiao Wang， Changjian Wang[1, 2] and Xing Wang[1]

[1] **School of Civil Engineering, Hefei University of Technology, Hefei 230009, PR China, chjwang@hfut.edu.cn**

[2] **Anhui International Joint Research Center on Hydrogen Safety, Hefei 230009, China**

ABSTRACT

Hydrogen is one of the promising energy sources in the future, because it has the advantages of clean combustion products, high efficiency, and renewable energy. However, hydrogen has the characteristics of low ignition energy, wide flammable range (4% -75%), and fast burning flame speed, which can cause explosion hazards. Typically, the accidental release of hydrogen into confined or semi confined enclosures can often lead to a flammable hydrogen-air mixture with concentration gradients and possible flame acceleration and deflagration-to-detonation transition (DDT). The present study aims to test the capability of our in-house density-based solver, ExplosionEngFoam, for flame acceleration (FA) and deflagration-to-detonation transition (DDT) in homogenous/inhomogeneous hydrogen-air mixtures. The solver is based on the open source computational fluid dynamics (CFD) platform OpenFOAM and uses the modified Weller et al.'s combustion model taking into account LD and RT instabilities, turbulence and non-unity Lewis number etc. Numerical simulations were conducted for both homogeneous and inhomogeneous mixtures in a long enclosed channel with 5.4 m in length and 0.06 m in height. The predictions demonstrate good quantitative agreement with the experimental measurements in flame tip position, speed and pressure profiles by Boeck et al. [1]. The flow characteristics such as flame fine structure, wave evolution etc. were also discussed.

Key words: Flame acceleration; Deflagration-to-detonation transition; Numerical simulation; Hydrogen safety

1. INTRODUCTION

Hydrogen is a kind of clean energy sources with a wide prospect of development [2, 3]. A booming demand of hydrogen energy requires a high degree of attention to the safety of generation, transportation, storage and consumption of hydrogen. The accidental release of hydrogen into confined or semi confined enclosures is an important issue for the safety of hydrogen, which can often lead to a flammable hydrogen-air mixture with concentration gradients and possible flame acceleration and deflagration-to-detonation transition (DDT) and cause explosion accident. It is necessary to investigate the process of possible flame acceleration and DDT for hydrogen explosion in enclosed space.

Numerous investigations both numerical and experimental have been conducted to study on hydrogen explosion, including flame propagation, deflagration to detonation and related

influential parameters in the past few years [4-8]. Boeck et al. [9] presented a discussion on the effect of transverse concentration gradients on detonation propagation through hydrogen-air explosion experiment in a closed rectangular channel. It was found that mixture with transverse concentration gradients was accompanied by a lower detonation propagation velocity compared to same concentration mixture in homogeneous case. The potential hazard of hydrogen-air mixtures has been studied in experiments by Vollmer et al. [10]. The experimental study has been conducted for different hydrogen concentration, concentration gradient, and obstacles with differing blockage ratio and spacing. The rationality of 7λ criterion for DDT prediction in homogeneous mixture was validated in their work. Heidari et al. [11] developed two detonation solvers, one based on the solution of the reactive Euler equations and another based on the programmed CJ burn method, to investigate the mechanism of transition from deflagration to detonation and find some valuable information. A further study was conducted for simulation of flame propagation and acceleration and transition from deflagration to detonation, and the effect of initial ignition strength was also investigated in their work [12]. Wang et al. [13] developed a density-based solver with single-step chemistry for hydrogen-air reaction to simulate flame acceleration and transition from deflagration to detonation. Azadboni et al. [14, 15] conducted numerical study within the OpenFOAM platform. The effect of concentration gradients on DDT was investigated.

The physical understanding and quantitative description of FA and DDT are still critically needed. Numerical simulation would be an economical and efficient approach. Combustion in configuration with a large aspect ratio such as channels, tunnels and pipes, especially in obstructed conditions, is expected to be more potential to spontaneous flame acceleration and transition from deflagration to detonation [16, 17]. A numerical code for 2D simulation of hydrogen-air explosion in a long closed channel is proposed in this paper， which aims to test the capability of our in-house density-based solver, Explosion Foam, for flame acceleration (FA) and deflagration-to-detonation transition (DDT) in homogenous/inhomogeneous hydrogen-air mixtures. In order to verify the reliability and accuracy of the numerical approach, the results of simulation are compared against the experimental work which is available in the literature.

2. NUMERICAL MODEL

2.1 Governing equations

Both reactants and products are assumed to behave as ideal gases in the model. The flow is governed by the compressible reactive Navier-Stokes equations and it can be written as follows:

$$\frac{\partial \rho}{\partial t} + \nabla \cdot \left(\rho \vec{U}\right) = 0 \tag{1}$$

$$\frac{\partial \rho \vec{U}}{\partial t} + \nabla \cdot \left(\rho \overrightarrow{UU}\right) + \nabla \cdot p = \nabla \cdot \tau \tag{2}$$

$$\frac{\partial \rho E}{\partial t} + \nabla \cdot \left(\rho \vec{U} E\right) + \nabla \cdot \left(\vec{U} p\right) = \nabla \cdot \left(\tau \cdot \vec{U}\right) + \nabla \cdot (\lambda \nabla T) + \nabla \cdot \left(\sum_{k=1}^{NS} \rho D h_k \nabla Y_k\right) \tag{3}$$

In the equations above, ρ, p, $\vec{\mathrm{U}}$, E, and Y_k are, respectively, the density, pressure, velocity,

total internal energy, and enthalpy and mass fraction of the kth species. t is time, τ is stress tensor, h_k is the specific enthalpy of kth species and NS is species number. D and λ are mass diffusion coefficient and conductivity coefficient, respectively.

The combustion process is described by the reaction process variable c. c= 0 corresponds to the unburned gas while c = 1 corresponds to the fully burned gas. The transport equation of the reaction process variable c can be expressed as:

$$\frac{\partial(\rho c)}{\partial t} + \nabla \cdot \left(\rho \vec{U} c\right) - \nabla \cdot (\rho D \nabla c) = \omega_c \tag{4}$$

The Weller combustion model [18] was employed to account for the deflagrative terms, together with a quenching factor of turbulent flames, $0 \le G \le 1$[19].

$$\omega_c = \rho_u \Sigma s_L |\nabla c| G \tag{5}$$

where S_L and ρ_u denote laminar burning speed and the density of the unburnt mixture.

As Bauwens et al. [20] suggested, the flame wrinkle factor Σ should be calculated as

$$\Sigma = \Sigma_t \times \Sigma_{LD} \times \Sigma_{RT} \tag{6}$$

where Σ_t , Σ_{LD} and Σ_{RT} denote the flame wrinkle factors caused by turbulence, Darrieuse-Landau (DL) and Rayleigh-Taylor (RT) instabilities, respectively.

The transport equation model closure for the flame wrinkle factor Σ_t is given as

$$\frac{\partial}{\partial t}\left(\rho \Sigma_t\right) + \frac{\partial}{\partial x_j}\left(\rho \Sigma_t u_j\right) = \frac{\partial}{\partial x_j}\left(\rho D_{eff} \frac{\partial \Sigma_t}{\partial x_j}\right) + \rho P_{\Sigma_t} \Sigma_t - \rho R_{\Sigma_t} \Sigma_t^{\,2} \tag{7}$$

where

$$P_{\Sigma_t} = 0.28 \sqrt{C_{u'}^3 \frac{\varepsilon}{\nu_u}} \tag{8}$$

$$R_{\Sigma_t} = \frac{P_{\Sigma_t}}{\Sigma_{eq}} \tag{9}$$

$$\Sigma_{eq} = 1 + C_\xi \left(1 + 2C_S\left(c - 0.5\right)\right) \sqrt{\frac{u'}{s_L}}\, \mathrm{Re}_\eta \tag{10}$$

$$\mathrm{Re}_\eta = \frac{u'}{\left(C_{u'} \nu_u \varepsilon\right)^{1/4}} \tag{11}$$

where $C_{u'} = 1$, $C_\xi = 0.62$ and $C_S = 1.\nu_u$, ε and u' are kinematic viscosity, the turbulence dissipation rate and the root-mean-square velocity, respectively.

The Darrieuse-Landau and thermo diffusive instabilities are modelled considering the expression as [20]

$$\Xi_{DL} = \max[1, \alpha_1 \left(\frac{\Delta}{\lambda_c}\right)^{1/3}] \tag{12}$$

where, λ_c, α_1 and Δ are cutoff wavelength of unstable scales, a coefficient to uncertainty in λ_c and the filter size, respectively.

The Rayleigh-Taylor instability is modelled as

$$\frac{\partial \bar{\rho} \Xi_{RT}}{\partial t} + \widehat{U}_s . \nabla \Xi_{RT} = \bar{\rho} G_{RT}(\Xi_{RT} - 1) - \bar{\rho} R_{RT}(\Xi_{RT} - 1) \tag{13}$$

where, $G_{RT}(\Xi_{RT} - 1)$ and $R_{RT}(\Xi_{RT} - 1)$ are rate of generation and removal of sub-grid wrinkling owing to RT-instability.

The coefficients G_{RT} and R_{RT} are modelled as

$$G_{RT} = 2\left(k_{RT} \frac{\sigma - 1}{\sigma + 1} \vec{a} . \vec{n}_f\right)^{1/2} \; and \; R_{RT} = \frac{8 \sigma S_L k_{RT}}{\pi} \tag{14}$$

where 'a' is flame acceleration, σ is flame expansion ratio, k_{RT} is unstable wavenumber associated with the RT-instability.

2.2 Numerical methods

In our group, an explosion simulation software, ExplosionEngFoam, was developed to solve the above Navier-Stokes equations using the finite volume method in OpenFOAM framework. The convection term can be solved by Harten-Lax-van-Leer-contact (HLLC) scheme [21-25]. Crank-Nicholson second-order scheme was employed for time terms while the second order central difference scheme was used for the diffusion term.

3. NUMERICAL SETUP

In this paper, the numerical simulations were conducted in a long closed channel with 5.4 m in length and 0.06 m in height for both obstructed and smooth channel with homogeneous and inhomogeneous mixtures, which mimics Boeck et al.'s [1]. The case of 30% blockage ratio (Br=2h/H) were considered for the obstructed channel. Simultaneously, seven groups of obstacles with height h are installed on the top and bottom walls of the explosion channel, as shown Fig. 1(a). The obstacle space is 300 mm. The first obstacle is located at x = 250mm, and the last obstacle is located at x = 2.05 m. The smooth channel is shown in Fig. 1(b), with same height and length as the obstructed channel. The hydrogen mole fraction for both homogenous and inhomogeneous mixture was 35%. The hydrogen concentration distribution for the inhomogeneous mixture is shown in Fig. 2. The initial condition for the mixture was 1atm and 293 K. In order to initiate the ignition, a patch with a radius of 5 mm at the ignition point (x = 0, y = 0 m) was set with an adiabatic flame temperature of 2448 K and one atmospheric pressure.

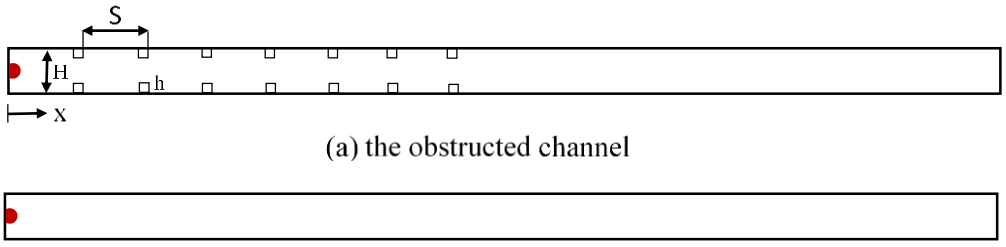

(a) the obstructed channel

(b) the smooth channel

Fig.1. Schematic of the computational domain

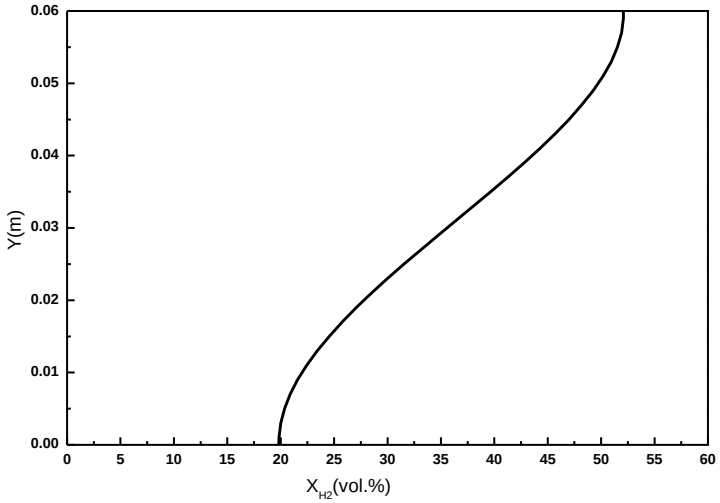

Fig.2. Distribution of vertical concentration in the channel for 35% hydrogen-air mixture

4. RESULTS AND DISCUSSIONS

Fig. 3 presents the comparison between predicted and measured flame tip position of 35% homogeneous hydrogen-air mixture for both obstructed channel and smooth channel. Fig. 4 and Fig.5 show the relationship between flame velocity and flame tip position of 35% homogenous/inhomogeneous hydrogen-air mixture both for smooth channel and obstructed channel. It is easy to find a reasonable agreement between the predicted and measured values. In the initial stage of flame propagation, the flame propagates with a slow speed of around several meters per second. A great amount of heat is produced companied with the combustion of hydrogen-air mixture, which results in a volume expansion and a flame acceleration. Then, the flame propagates with a bigger flame acceleration and even reaches a high speed of more than 2000m/s.

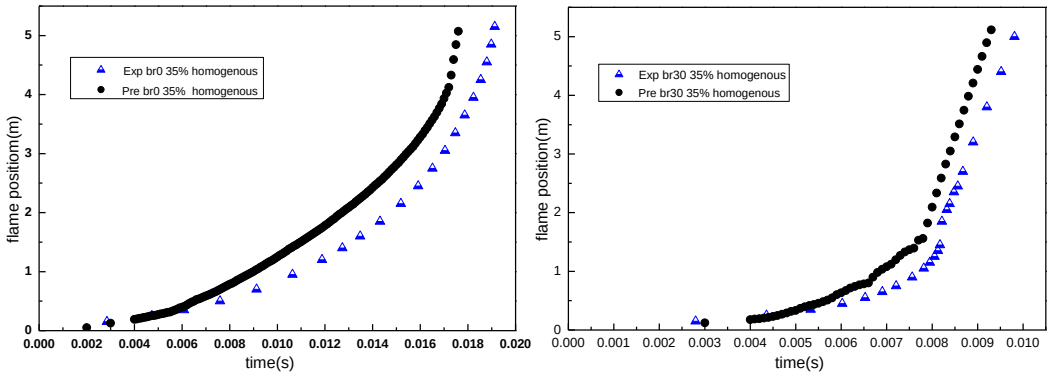

Fig.3. Comparison between the predicted and measured flame tip positions for the homogenous mixture in smooth (left) and obstructed (right) channels

Homogenous/inhomogeneous mixture flame velocities from experiments and numerical simulations are compared in Fig.4 and Fig.5. Fig.4 is for smooth channel while Fig.5 is for obstructed channel (Br=30%). The simulation results are in reasonably good agreement with experimental results. It can be seen that the concentration gradient has a significant effect on flame speed in the smooth channel, and as a result the flame speed increases faster in inhomogeneous mixture and achieve the transition to detonation in an earlier time than that in homogenous mixture. The effect of concentration gradient on flame speed in obstructed channel is not obvious.

For the smooth channel with the homogeneous or inhomogeneous mixture, the flame tip velocity initially increases by degrees, which results in the enhancement of turbulence, LD and RT instabilities. These exert a positive feedback to the flame. Resultantly, the flame speed increases continuously and accelerates sharply around the location of x=4.0m.

For the obstructed channel with the homogeneous or inhomogeneous mixture, flame propagates with a bigger acceleration compared with the smooth channel. Flame speed increases fast and reaches values around 2000 m/s in the obstructed part (0 m < x < 2.05 m), indicating that the transition to detonation occurs here. With the presence of obstacles, the acceleration is extremely strong as compared to the unobstructed channel. On the one hand, the obstacles induce the generation of turbulence, LD and RT instabilities, consequently increase the flame surface which promotes the burning rate. On the other hand, obstacles provide a newly physical mechanism of flame acceleration, which is based on delayed burning between the obstacles, creating a strong jet-flow and thus causing acceleration [26]. The flame propagates fast along the unobstructed part of the channel, leaving behind some unburned mixture between the obstacles which are burned later. Delayed burning in the empty space between obstacles produces a strong jet flow in the unobstructed section of the channel. This jet flow causes a faster propagation of flame tip, which creates new delayed burning in front section and thereby brings a positive feedback between the flame and the flow, driving the flame to be accelerated. This flame acceleration mechanism can be powerful, causing supersonic flame propagation and then to transition from deflagration to detonation.

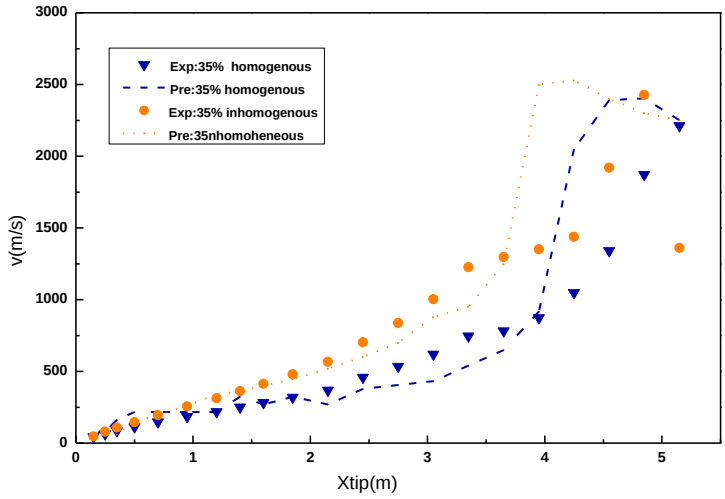

Fig.4. Comparison between the predicted and measured flame tip speed in the smooth channel

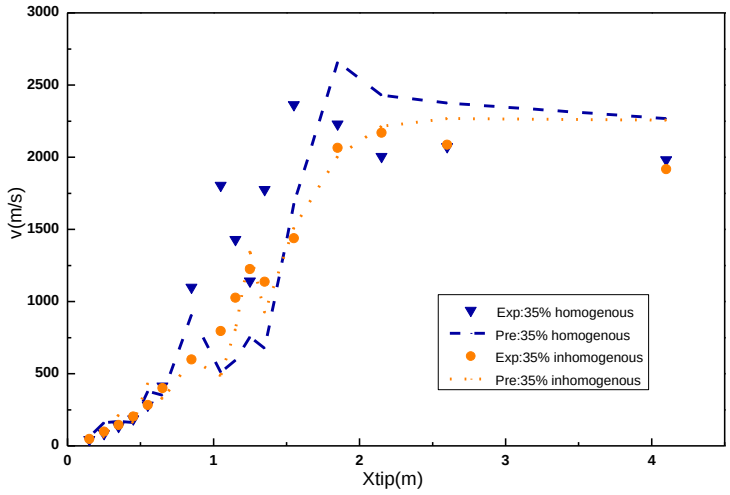

Fig.5. Comparison between the predicted and measured flame tip speed in the obstructed channel

Fig.6 presented the predicted and measured pressure histories at specified probe locations (x=o.4m, x=2.3m, x=3.2m, x=4.1m) for 35% homogenous hydrogen-air mixture in the obstructed channel (Br =30%). The simulated pressure profiles are consistent with the experimental data. Moreover, the predicted first pressure peak times at x=0.4m, 2.3m and 3.2m keep good agreement with the experimental results, while the predicted time for first peak pressure at position of 4.1 m are slightly earlier than the measured one. The simulated peak pressures are a little higher than experimental data, since the simulated flame detonation speed is about 10% faster than experimental result, and the time for deflagration to detonation are a little earlier than the experimental value.

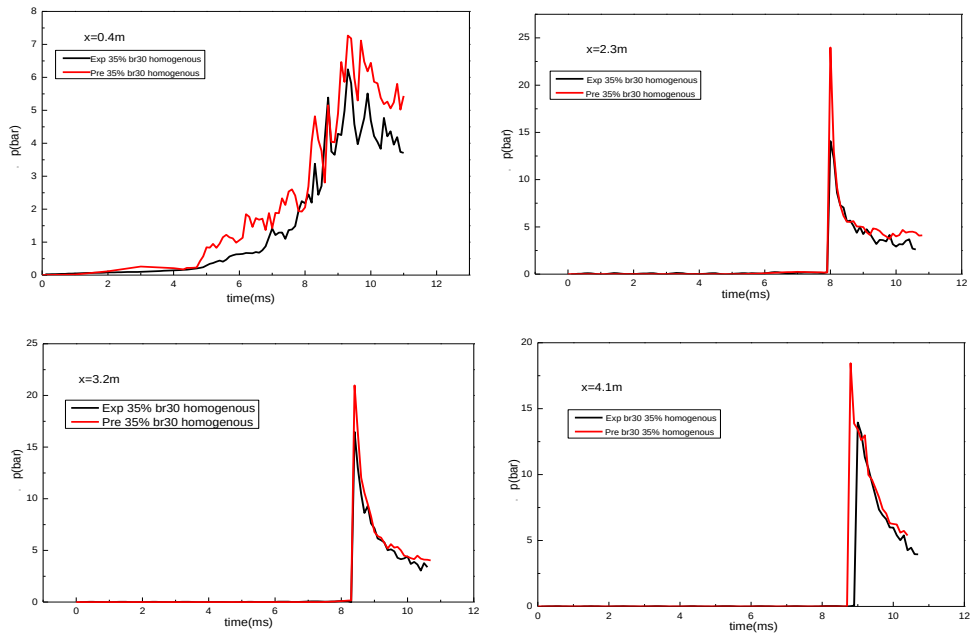

Fig.6. Comparison of the predicted and measured pressure profiles at specified probe locations(x=0.4m, x=2.3m, x=3.2m, x=4.1m).

Fig.7 shows the predicted contours of temperature during the initial flame propagation for 35% homogenous hydrogen-air mixture in obstructed channel (A) and smooth channel (B). At 4.1ms, the flame front keeps a shape of semicircle, and propagates at a slow laminar speed. Owing to the wave reflection at the obstacles, the flame propagation in obstructed channel is slower than that in smooth channel before first group of obstacles. At 4.5ms, the flame front wrinkles and twisted. The flame superficial area is increased, accompanied with a higher flame speed and stronger heat release, which is caused by intrinsic flow instabilities. As the presence of obstacles, flame accelerates faster in obstructed channel compared to smooth channel.

The predicted contours of temperature, pressure and H2 mass fraction during FA and DDT are presented in Fig.8, Fig.10 and Fig11 respectively for 35% inhomogeneous mixture. For the convenience of observation, the parts of the smooth channel in A (from x=0.85m to x= 2.2m) and the obstructed channel in B (from x=2.95m to x=4.3m) are shown. Comparison between contours of temperature in smooth channel and obstructed channel is shown in Fig.8. Before the transition to detonation, the preheating areas are visible ahead of the flame front both in smooth and obstructed channels. It indicates that the compressed wave generated by burning of mixture is ahead of the flame front and preheat the unburned mixture. At 16.5ms in smooth channel, a hot spot occurs near the location of 3.25m of the bottom wall, which results in a subsequent explosion. A new flame produced by the explosion propagate with a faster speed than the flame front. Then it crosses the flame front and achieves the transition to detonation in 16.8ms.

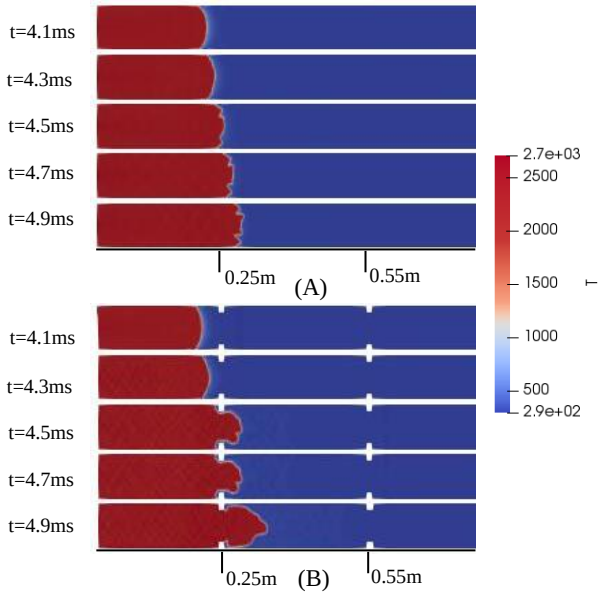

Fig.7. Predicted contours of temperature during the initial flame propagation

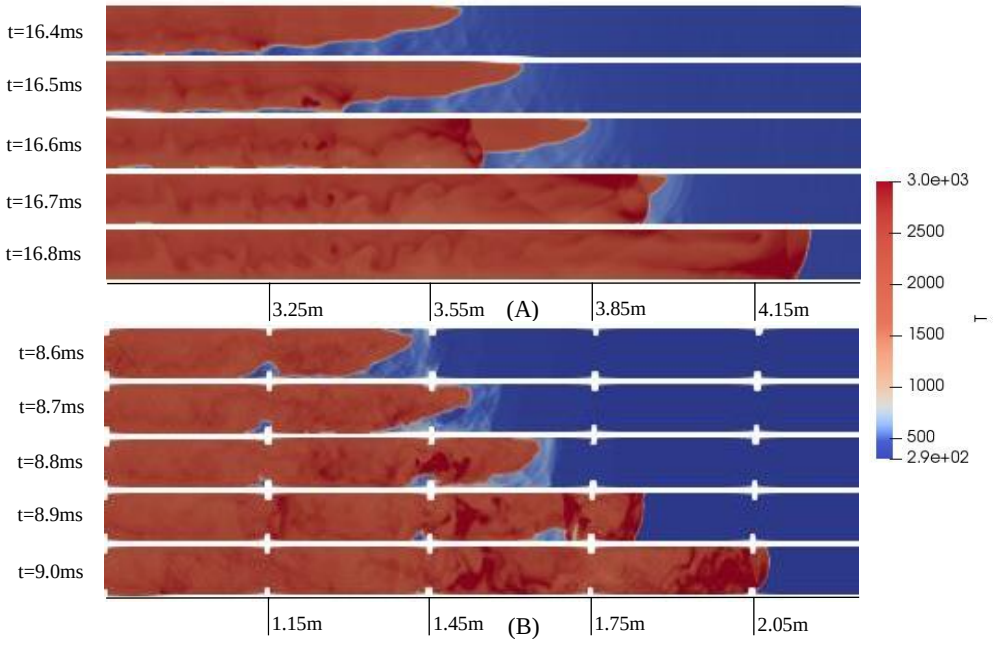

Fig.8. Comparison between the predicted contours of temperature of smooth channel and obstructed channel during FA and DDT

For the obstructed channel, the transition to detonation occurs much earlier, at 8.9ms. More details can be seen in Fig9. At 8.86ms, the interaction between the wave and obstacles induces a local ignition at the top of the sixth group of obstacles. At 8.87ms, a subsequent one occurs at bottom of the sixth group of obstacles. Resultantly the transition to detonation occurs.

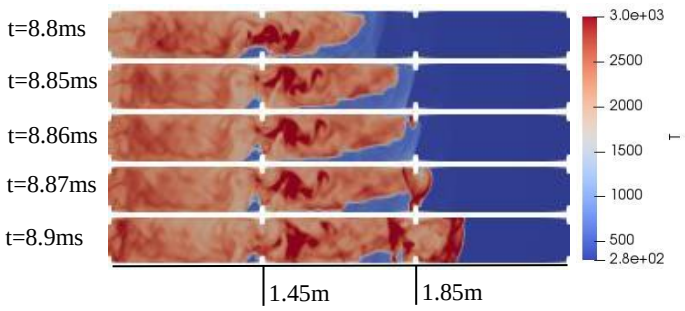

Fig.9. The predicted contours of temperature during DDT

As shown in Fig.10, an obvious high pressure region occurs in the bottom wall of the smooth channel at 16.5ms, corresponding to the hot spot in temperature contour. It is caused by the reflection of shock wave off the wall, which is accompanied with increase of temperature and pressure near the wall. The reflection of shock waves on the upper and bottom walls induces a powerful acceleration of the new flame and a wider high pressure region can be found in the smooth channel. The transition to detonation is completed at 16.8ms. For the obstructed channel, high regions occur near the obstacles, which is caused by the interaction between shock waves and obstacles. It plays a major role in driving the flame to detonation.

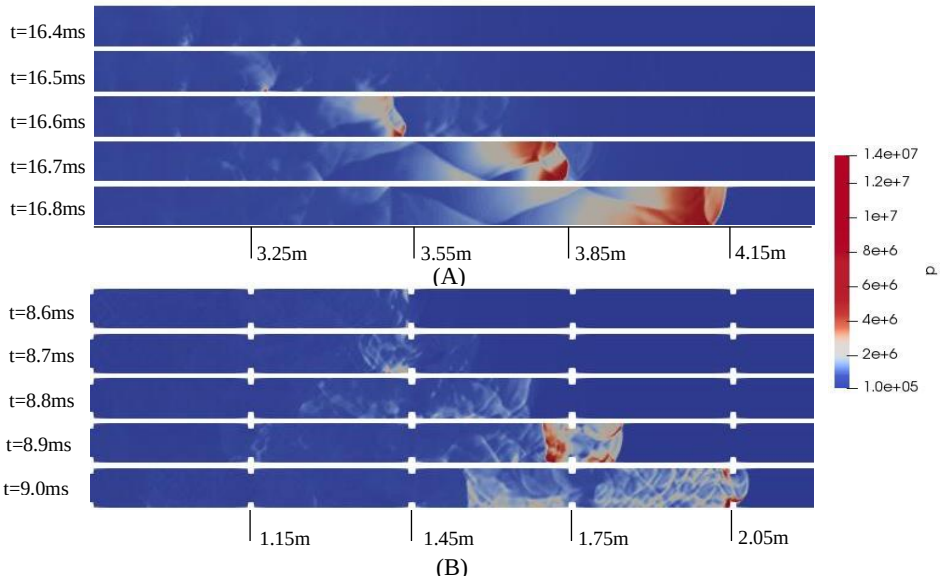

Fig.10. Comparison between the predicted contours of pressure of smooth channel and obstructed channel during FA and DDT

Fig11 presented the predicted contours of H_2 mass fractions. There are pairs of vortex ahead of the flame in the right of obstacles, which are caused by the interaction between obstacles and gas flow. Once the flame passes through these regions, the vortex pairs disappear, but the relatively high vertical hydrogen concentrations can still be found in the burned regions. However, no vortex can be seen ahead the flame front in the smooth channel. It indicates that the presence of vortex is caused by obstacles. The hydrogen concentration gradient can be still found in both smooth channel and obstructed channel in the burned regions. Since the

process from ignition to deflagration to detonation is fast as tens of ms, excess hydrogen remains in the upper part of the channel. This shows a risk can still exist in the burned area, which may result in a re-ignition once enough fresh air is available in an accidental scenario, causing secondary explosion accidents.

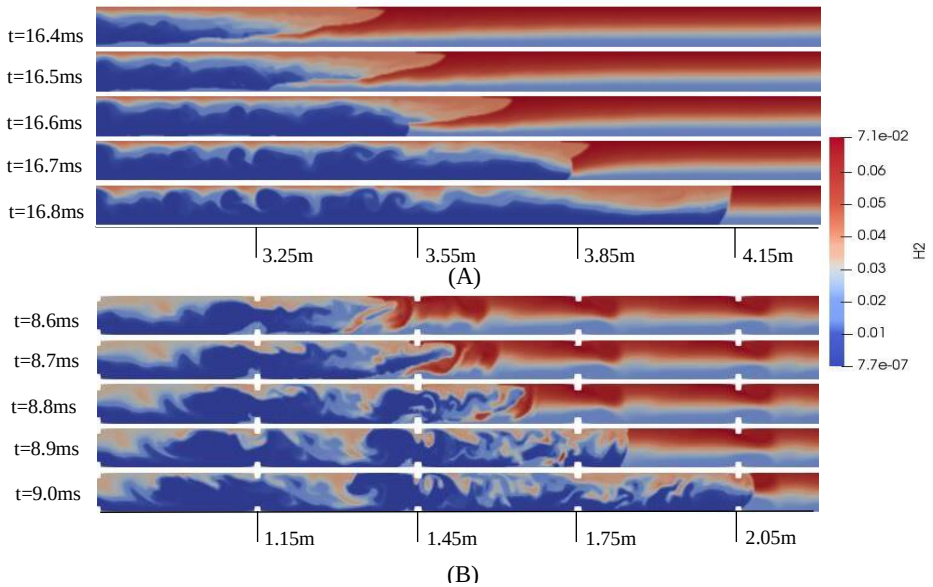

Fig.11. Comparison between the predicted contours of H_2 mass fractions of smooth channel and obstructed channel during FA and DDT

CONCLUSIONS

The in-house density-based solver, ExplosionFoam, for flame acceleration (FA) and deflagration-to-detonation transition (DDT) in homogenous/inhomogeneous hydrogen-air mixtures was developed in the OpenFOAM framework. The capability of the solver has been tested by the simulation of experiments available in the literature [1]. The predictions demonstrate good quantitative agreement with the experimental measurements in flame tip position, speed and pressure profiles by Boeck et al. [1].

The analysis shows that concentration gradient gives impetus to flame acceleration in the smooth channel while the effect of concentration gradient on flame acceleration and transition from deflagration to detonation is not obvious in obstructed channel. LD and RT instabilities and turbulence play an important role in FA. The physical mechanism of flame acceleration for obstacles in obstructed channel is discussed in the paper, taking account the wrinkle and jet flow which are caused by obstacles and result in flame acceleration. The details of flame acceleration and transition of deflagration to detonation have been discussed. Obstacles have an active influence on FA and DDT. DDT in obstructed channel occurs much earlier than that in smooth, as the effect of obstacles. The analysis on distribution of hydrogen concentration shows that the risk of secondary explosions still exists in burned area.

ACKNOWLEDGEMENTS

The authors gratefully acknowledge the National Key R&D Program of China (No.2016YFE0113400).

REFERENCES

[1] Boeck LR, Katzy P, Hasslberger J, Kink A, Sattelmayer T. The GraVent DDT database. Shock Waves. 2016;26(5):683-5.

[2] Parra D, Valverde L, Pino FJ, Patel MK. A review on the role, cost and value of hydrogen energy systems for deep decarbonisation. Renewable and Sustainable Energy Reviews. 2019;101:279-94.

[3] Ozawa A, Kudoh Y, Kitagawa N, Muramatsu R. Life cycle CO2 emissions from power generation using hydrogen energy carriers. International Journal of Hydrogen Energy. 2019.

[4] Oran ES, Gamezo VN. Origins of the deflagration-to-detonation transition in gas-phase combustion. Combustion and Flame. 2007;148(1-2):4-47.

[5] Na'inna AM, Phylaktou HN, Andrews GE. Effects of Obstacle Separation Distance on Gas Explosions: The Influence of Obstacle Blockage Ratio. Procedia Engineering. 2014;84:306-19.

[6] Zhu YJ, Chao J, Lee JHS. An experimental investigation of the propagation mechanism of critical deflagration waves that lead to the onset of detonation. Proceedings of the Combustion Institute. 2007;31(2):2455-62.

[7] Li Q, Sun X, Wang X, Zhang Z, Lu S, Wang C. Experimental study of flame propagation across flexible obstacles in a square cross-section channel. International Journal of Hydrogen Energy. 2019;44(7):3944-52.

[8] Aditya Karanam, Pavan K. Sharma, Ganju S. Numerical simulation and validation of flame acceleration and DDT in hydrogen air mixtures. International Journal of hydrogen Energ y. 2018;4 3:17492-504.

[9] Boeck LR, Berger FM, Hasslberger J, Sattelmayer T. Detonation propagation in hydrogen–air mixtures with transverse concentration gradients. Shock Waves. 2016;26(2):181-92.

[10] Vollmer KG, Ettner F, Sattelmayer T. Deflagration-to-Detonation Transition in Hydrogen/Air Mixtures with a Concentration Gradient. Combustion Science & Technology. 2012;184(10-11):1903-15.

[11] Heidari A, Wen JX. Flame acceleration and transition from deflagration to detonation in hydrogen explosions. International Journal of Hydrogen Energy. 2014;39(11):6184-200.

[12] Heidari A, Wen JX. Numerical simulation of flame acceleration and deflagration to detonation transition in hydrogen-air mixture. International Journal of Hydrogen Energy. 2014;39(36):21317-27.

[13] Wang CJ, Wen JX. Numerical simulation of flame acceleration and deflagration-to-detonation transition in hydrogen-air mixtures with concentration gradients. International Journal of Hydrogen Energy. 2016.

[14] Azadboni RK, Wen JX, Heidari A, Wang C. Numerical modeling of deflagration to detonation transition in inhomogeneous hydrogen/air mixtures. Journal of Loss Prevention in the Process Industries. 2017:S0950423017303935.

[15] Khodadadi Azadboni R, Heidari A, Boeck LR, Wen JX. The effect of concentration

gradients on deflagration-to-detonation transition in a rectangular channel with and without obstructions– A numerical study. International Journal of Hydrogen Energy. 2019;44(13):7032-40.
[16] Bychkov V, Valiev D, Eriksson LE. Physical mechanism of ultrafast flame acceleration. Phys Rev Lett. 2008;101(16):164501.
[17] Ju Y, Maruta K. Microscale combustion: Technology development and fundamental research. Progress in Energy and Combustion Science. 2011;37(6):669-715.
[18] H. G. Weller GT, A. D. Gosman and C. Fureby. Application of a flame-wrinkling LES combustion model to a turbulent mixing layer. Twenty-Seventh Symposium (International) on Combustion/The Combustion Institute1998. p. 899-907.
[19] V. L. Zimont ANL. A numerical model of premixed turbulent combustion of premixed gases. Chemical Physics Reports. 1995;14:993-1025.
[20] Bauwens CR, Chaffee J, Dorofeev SB. Vented explosion overpressures from combustion of hydrogen and hydrocarbon mixtures. International Journal of Hydrogen Energy. 2011;36(3):2329-36.
[21] Vaagsaether K, Knudsen V, Bjerketvedt D. Simulation of flame acceleration and DDT in H2H2-air mixture with a flux limiter centered method. International Journal of Hydrogen Energy. 2007;32(13):2186-91.
[22] I YP, Chiu YL, Wu SJ. The simulation of air recirculation and fire/explosion phenomena within a semiconductor factory. Journal of hazardous materials. 2009;163(2-3):1040-51.
[23] Rocourt X, Gillard P, Sochet I, Piton D, Prigent A. Thermal degradation of two liquid fuels and detonation tests for pulse detonation engine studies. Shock Waves. 2006;16(3):233-45.
[24] Barlow AJ, Roe PL. A cell centred Lagrangian Godunov scheme for shock hydrodynamics. Computers & Fluids. 2011;46(1):133-6.
[25] Qu F, Yan C, Yu J, Sun D. A new flux splitting scheme for the Euler equations. Computers & Fluids. 2014;102:203-14.
[26] Bychkov V, Akkerman Vy, Valiev D, Law CK. Influence of gas compression on flame acceleration in channels with obstacles. Combustion and Flame. 2010;157(10):2008-11.